Cell Reports

Resource

The Self-Inactivating KamiCas9 System for the Editing of CNS Disease Genes

Graphical Abstract

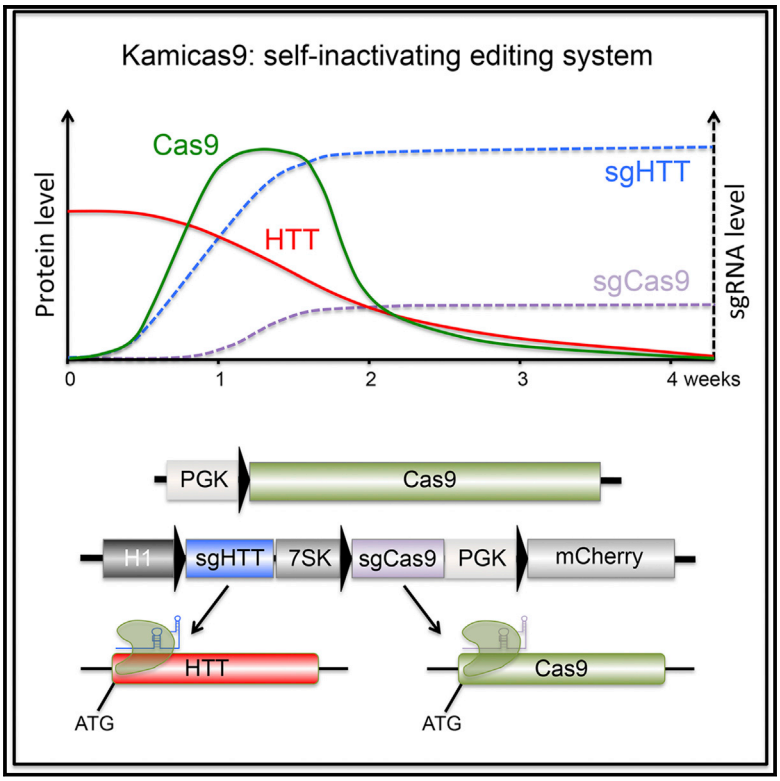

Highlights

- KamiCas9 allows for transient nuclease expression and improved editing safety
- Highly efficient genome editing in neuronal and glial cells of the brain
- Huntington's disease pathological hallmarks improve with huntingtin disruption

Authors

Nicolas Merienne, Gabriel Vachey, Lucie de Longprez, ..., Anselme L. Perrier, Renaud du Pasquier, Nicole Déglon

Correspondence

nicole.deglon@chuv.ch

In Brief

Merienne et al. describe the KamiCas9 method, a self-inactivating system for transient genome editing with improved safety. They demonstrate the feasibility and impact in the CNS with the permanent disruption of huntingtin gene in the context of Huntington's disease.

Merienne et al., 2017, Cell Reports *20*, 2980–2991
September 19, 2017
http://dx.doi.org/10.1016/j.celrep.2017.08.075

CellPress

OPEN ACCESS
CellPress

Cell Reports
Resource

The Self-Inactivating KamiCas9 System for the Editing of CNS Disease Genes

Nicolas Merienne,[1,2,10] Gabriel Vachey,[1,2,10] Lucie de Longprez,[3,4] Cécile Meunier,[5] Virginie Zimmer,[1,2] Guillaume Perriard,[6,7] Mathieu Canales,[6,7] Amandine Mathias,[6,7] Lucas Herrgott,[1,2] Tim Beltraminelli,[1,2] Axelle Maulet,[8] Thomas Dequesne,[1,2] Catherine Pythoud,[1,2] Maria Rey,[1,2] Luc Pellerin,[5] Emmanuel Brouillet,[3,4] Anselme L. Perrier,[8] Renaud du Pasquier,[6,7,9] and Nicole Déglon[1,2,11,*]

[1]Department of Clinical Neurosciences, Laboratory of Cellular and Molecular Neurotherapies (LCMN), Lausanne University Hospital, 1011 Lausanne, Switzerland
[2]Neurosciences Research Center (CRN), LCMN, Lausanne University Hospital, 1011 Lausanne, Switzerland
[3]CEA, DRF, Institut François Jacob, Molecular Imaging Research Center (MIRCen), F-92265 Fontenay-aux-Roses, France
[4]Neurodegenerative Diseases Laboratory, CNRS, CEA, Université Paris-Sud, Université Paris-Saclay (UMR9199), F-92265 Fontenay-aux-Roses, France
[5]Department of Physiology, Laboratory of Neuroenergetics, University of Lausanne, 1011 Lausanne, Switzerland
[6]Department of Clinical Neurosciences, Laboratory of Neuro-immunology, Lausanne University Hospital, 1011 Lausanne, Switzerland
[7]Neurosciences Research Center (CRN), Laboratory of Neuro-immunology, Lausanne University Hospital, 1011 Lausanne, Switzerland
[8]Institut National de la Santé et de la Recherche Médicale (INSERM) UMR861, I-Stem, AFM, 91100 Corbeil-Essonnes, France
[9]Service of Neurology, Department of Clinical Neurosciences, Lausanne University Hospital, 1011 Lausanne, Switzerland
[10]These authors contributed equally
[11]Lead Contact
*Correspondence: nicole.deglon@chuv.ch
http://dx.doi.org/10.1016/j.celrep.2017.08.075

SUMMARY

Neurodegenerative disorders are a major public health problem because of the high frequency of these diseases. Genome editing with the CRISPR/Cas9 system is making it possible to modify the sequence of genes linked to these disorders. We designed the KamiCas9 self-inactivating editing system to achieve transient expression of the Cas9 protein and high editing efficiency. In the first application, the gene responsible for Huntington's disease (HD) was targeted in adult mouse neuronal and glial cells. Mutant huntingtin (HTT) was efficiently inactivated in mouse models of HD, leading to an improvement in key markers of the disease. Sequencing of potential off-targets with the constitutive Cas9 system in differentiated human iPSC revealed a very low incidence with only one site above background level. This off-target frequency was significantly reduced with the KamiCas9 system. These results demonstrate the potential of the self-inactivating CRISPR/Cas9 editing for applications in the context of neurodegenerative diseases.

INTRODUCTION

Neurodegenerative diseases are a major public health issue and they pose a difficult challenge in medicine. They are the leading cause of age-related chronic diseases, and their prevalence is rapidly increasing with changes in the population, including greater life expectancy (Wu et al., 2016). These diseases result from monogenic mutations or from a combination of multiple genetic and aged-related risk factors in given environmental conditions, and their underlying pathophysiological mechanisms are complex. Symptoms generally begin in adulthood and the manipulation of genes linked to these disorders in post-mitotic adult cells. It is challenging to improve our understanding of these conditions or to target the causal genes for treatment (Izpisua Belmonte et al., 2015; Yang et al., 2016).

Huntington's disease (HD) is a well-characterized pathology, which could be used as a representative neurodegenerative disorder to improve current therapeutic approaches. HD is caused by a single genetic mutation on exon 1 of the huntingtin (*HTT*) gene, conferring a selective vulnerability of striatal spiny projecting neurons (Bates et al., 2015). Currently, there is no treatment for HD. Considering that the mutation is a toxic gain-of-function, a promising approach would be to decrease the expression level of the mutant *HTT* (Ross and Tabrizi, 2011). This has been already achieved with the use of RNA silencing tools, which demonstrated that a partial mutant *HTT* knockdown is sufficient to induce long-term decreases in mutant *HTT*-positive aggregates, behavioral improvements, and reduction of neuronal dysfunction and death (Boudreau et al., 2009; Cambon et al., 2017; Drouet et al., 2009; Southwell et al., 2012). This approach is currently under evaluation in a phase I/II clinical trial with antisense oligonucleotides (Smith et al., 2016). However, RNA silencing only provides a partial and transient *HTT* suppression, and an approach ensuring a complete and permanent *HTT* disruption would be preferable. This can be achieved with genome-editing technologies, in particular the recently characterized CRISPR/Cas9 system.

The CRISPR/Cas9 system is a powerful new technology in which the Cas9 nuclease is directed to a specific genomic region with a single-guide RNA (sgRNA) (Mali et al., 2013; Shalem et al.,

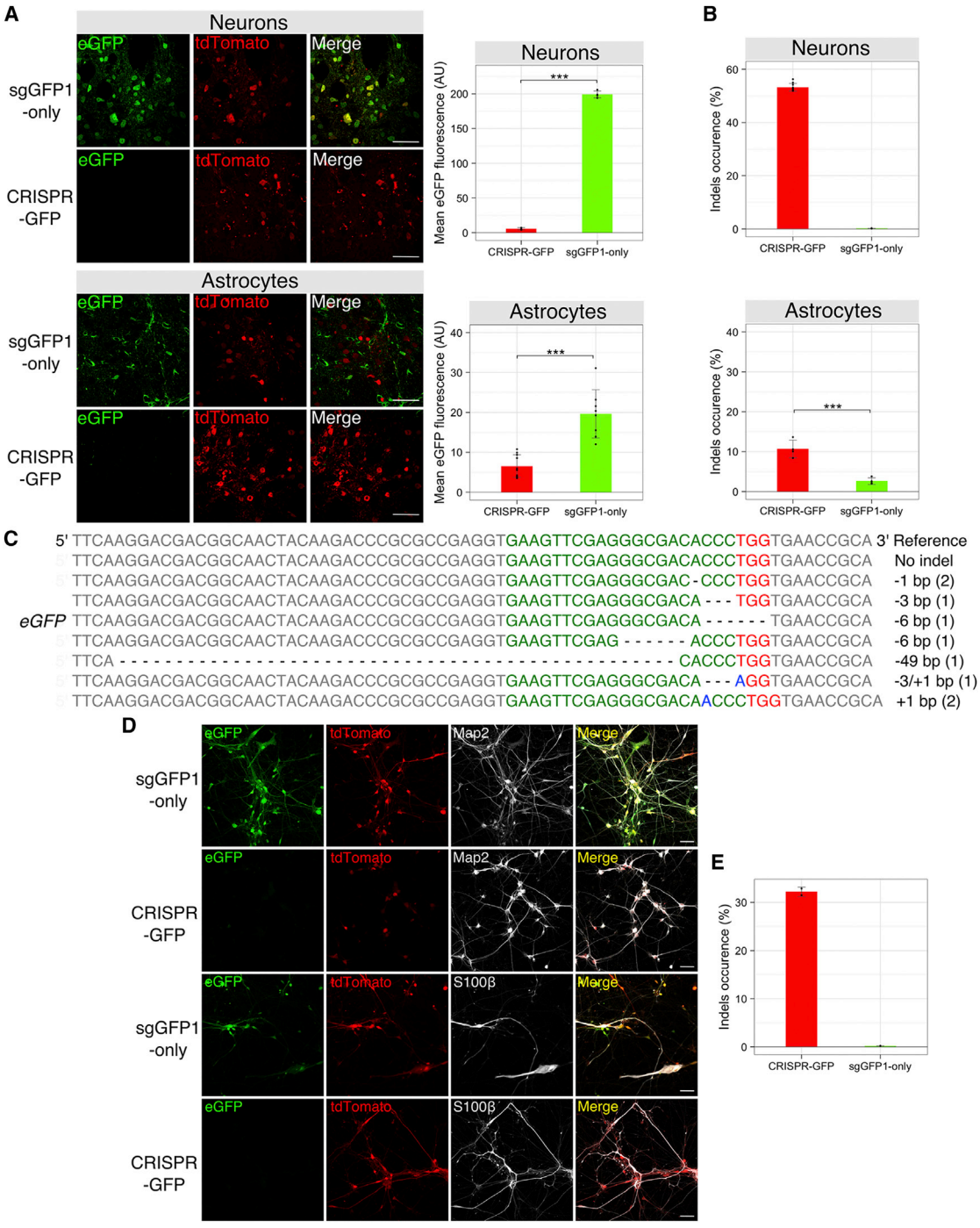

Figure 1. Evaluation of In Vivo Genome Editing in Striatal Neuronal and Glial Cells and in Human Neurons Derived from iPSCs

(A) Confocal acquisitions (left) and mean eGFP fluorescence intensity quantifications (right), 4 weeks post-infection, revealed significantly lower levels of eGFP fluorescence in mouse striatal neurons (up, CRISPR-GFP: n = 4; sgGFP1-only, n = 4) and astrocytes (down, CRISPR-GFP: n = 10; sgGFP1-only, n = 8) infected with CRISPR-GFP than in controls (sgGFP1-only).

(B) Genomic DNA from the injected area was extracted, and the *eGFP* cassette was amplified by PCR to check for indels. Surveyor analysis showed that *eGFP* was efficiently edited in both cell types (neurons, CRISPR-GFP: n = 10, sgGFP1-only, n = 8; astrocytes, CRISPR-GFP: n = 4, sgGFP1-only, n = 4).

(C) *eGFP* PCR products from one CRISPR-GFP sample were inserted into a plasmid for Sanger sequencing. Nine of the *eGFP* sequences analyzed contained indels.

(legend continued on next page)

2015) to cleave the DNA target sequence. This system has been successfully used to correct mutations in genetic diseases of peripheral organs and to target genes in the brain (Kolli et al., 2017; Long et al., 2016; Monteys et al., 2017; Nelson et al., 2016; Shin et al., 2016, 2017; Swiech et al., 2015; Tabebordbar et al., 2016). One major challenge for CNS applications is the development of a system allowing transient expression of the Cas9 nuclease in order to improve the biosafety and limit off-target events. Here, we developed the KamiCas9 self-inactivating system ensuring transient expression of the Cas9 protein with on-target performance similar to CRISPR/Cas9. We used the non-homologous end-joining (NHEJ) pathway, active in post-mitotic cells, to inactivate the gene implicated in HD and demonstrate high *HTT* editing in neurons derived from HD-induced pluripotent stem cells (iPSCs) and in the striatum of mice. *HTT* inactivation was associated with a drastic reduction of *HTT* aggregate formation and reduced neuronal dysfunctions, confirming the potential of the approach. Finally, sequencing demonstrates low off-target incidence, which is further decreased when KamiCas9 is used to target *HTT*.

RESULTS

We took advantage of the large cloning capacity of lentiviral vectors (LV) and their high transduction efficiencies, safety, and long-term expression in the CNS to optimize the CRISPR/Cas9 system delivery (Cartier et al., 2009; Jarraya et al., 2009; Naldini et al., 1996). We first assessed the system in human embryonic kidney 293T (HEK293T) cells carrying various copies of an artificial mCherry-eGFP target sequence (Figure S1). The sequence of the mCherry reporter gene is followed by a target sequence (sgTARGET) containing a stop codon and finally a GFP reporter gene (Figure S1A). In the control condition, only the mCherry reporter gene was expressed, whereas gene editing by the sgTARGET destroyed the stop codon and rescue GFP expression (Figures S1A and S1F). To characterize the kinetic and potential limiting factors, we generated TARGET-IP HEK293T cell populations with 12, 32, 52, and 91 integrated sequences in their genomes (Figures S1B and S1C) and examined the kinetics of the reaction and importance of Cas9:sgRNA ratio on indels efficiency (Figures S1D and S1E). These experiments revealed that a 1:1 ratio between Cas9:sgRNA is optimal and that the number of target sequences is affecting the kinetics of genome editing, but not the final efficiency, which reached a plateau in all conditions after 10–14 days, as expected from the biology of CRISPR/Cas9 (Figures S1D–S1F).

Based on these initial evaluations, we next assessed the editing efficiency of the enhanced green fluorescent protein (eGFP) gene in mouse primary cultures (Figure S2). Cortical neurons or astrocytes were infected with LV expressing eGFP, Cas9, and tdTomato-sgGFP1, or as negative control with LV-eGFP and LV-tdTomato-sgGFP1 (Figure S2). In the control group, a large proportion of the cells co-expressed the GFP and tdTomato reporter genes (Figures S2E, S2G, and S2I). In contrast, the mean eGFP fluorescence intensity was reduced in CRISPR-edited cells with a large proportion of tdTomato-positive and GFP-negative cells (Figures S2D, S2F, and S2H). To exclude biases in the experimental conditions, we measured eGFP protein by western blot and showed equivalent expression levels in both groups (data not shown). Quantification of indels in cortical neuron (Figure S2B) and astrocyte cultures (Figure S2C) with the Surveyor assay (Cong et al., 2013) corroborated these results and demonstrated the high efficiency and reproducibility of GFP editing.

High in vivo editing is a crucial parameter for the development of CNS editing and to reach therapeutic benefits. We therefore performed a proof-of-principle GFP editing study in striatal cell-types affected in HD (Ross and Tabrizi, 2011). LV-Cas9 and LV-sgRNA were premixed in equal amounts and striatal neurons and astrocytes were transduced with vectors specifically targeting these cells. The neuronal tropism was obtained with VSV-G-pseudotyped LV and a phosphoglycerate kinase promoter driving the expression of the transgene (Déglon et al, 2000). Microscopy observations showed a large number of neurons expressing the mCherry fluorescent protein present in the vector expressing the guide RNA (Figures S3A and S3B). This result confirms the high transduction efficiency of LV in the CNS (100,000–150,000 infected cells in the striatum with a single injection of LV (Colin et al., 2009; de Almeida et al., 2002). For the glial targeting, the GfaABC1D(B)3 promoter derived from the GFAP promoter and a miR124T detargeting sequence were used (Figure S4) (Colin et al., 2009; de Leeuw et al., 2006; Merienne et al., 2013). Mosaic acquisitions and eGFP fluorescence intensity quantifications revealed a strong loss of fluorescence in the neurons (97%) or astrocytes (67%) of the CRISPR-GFP groups (Figure 1A). No alteration of the striatal markers NeuN and DARPP-32 (Bibb et al., 2000; Luthi-Carter et al., 2000; Ouimet et al., 1998; van Dellen et al., 2000) or reporter gene expression was detected, confirming the absence of impact of LVs and Cas9 expression in the brain (Figure S3A). Surveyor analysis on whole striatal tissues from these animals indicated that about 50% of the neurons and 15% of the astrocytes had undergone editing (Figure 1B). The difference between neurons and astrocytes reflects a bias due to the relative number of neuronal and glial cells (>70% neurons; unpublished data) in the striatum (Figure S3D) and additional caveats. In particular, the presence of transduced and non-transduced cells in the striatal punches (Figure S3D) and the fact that if editing frequency is sufficiently high, mutated sequences in homoduplexes are not detected by the Surveyor assay, leading to an underestimation of editing, as previously reported (Nelson et al., 2016). The Sanger sequencing around the target site confirmed this interpretation and indicated that eGFP editing in neurons occurred in 9 out of the 10 clones analyzed (Figure 1C). Finally, we tested the CRISPR/Cas9 system on co-cultured human neurons and glial

(D) Evaluation of *eGFP* editing in human neurons derived from induced pluripotent stem cells (iPSCs), demonstrating much lower levels of eGFP fluorescence in the CRISPR-GFP group (n = 3, N = 2) than in controls (n = 3, N = 2) in MAP2-positive (neurons) and S100β-positive (astrocytes) cells.
(E) Surveyor analysis on the *eGFP* sequence confirmed the presence of indels in the CRISPR-GFP group (n = 2, N = 1). AU: arbitrary units; bp: base pair. The results are presented as mean ± SD. ***$p < 0.001$. Scale bar, 50 μm.
See also Figures S3–S5.

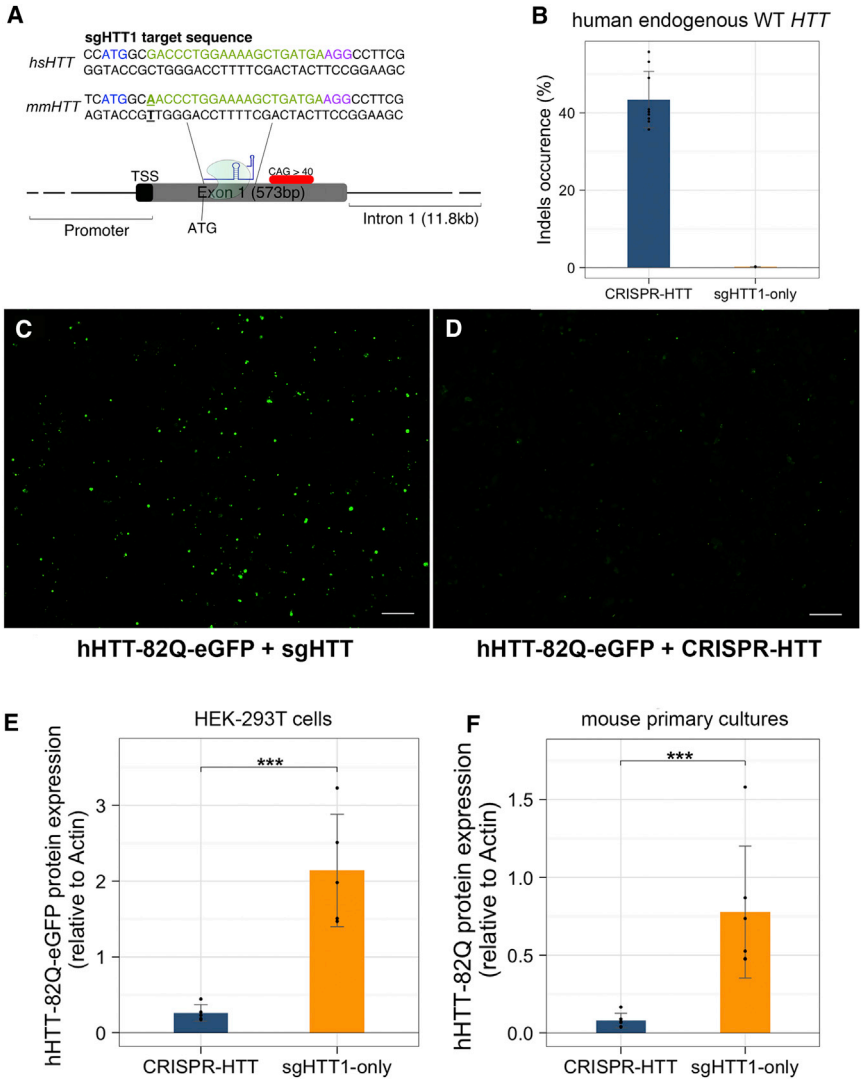

Figure 2. Human *HTT* Editing in HEK293T Cells and Primary Cultures

(A) Schematic representation of the location of the sgHTT1 target site in the human (*hHTT*) and endogenous mouse (*mmHTT*) *HTT* genes. Blue: *HTT* translation start site; green: sgHTT1 binding site; red: PAM, bold-underlined nucleotide represents mismatch between sgHTT1 and the target sequence.

(B) Efficiency of human endogenous *HTT* (*hHTT*) editing in HEK293T cells. HEK293T cells were transfected with plasmids encoding Cas9 and sgHTT1 (CRISPR-HTT, n = 9, N = 2) or sgHTT1 alone (sgHTT1-only, n = 7, N = 2). Surveyor assays showed that *hHTT* was efficiently edited in the CRISPR-HTT group 7 days post-transfection.

(C and D) Direct fluorescence acquisitions revealed the presence of a large number of eGFP-positive mutant HTT aggregates in the sgHTT1-only group (C) (n = 3, N = 1), and much lower levels of HTT aggregation in the CRISPR-HTT group (D) (n = 3, N = 1) 7 days post-transfection.

(E) HEK293T cells were transfected with plasmids encoding Cas9, sgHTT1, and a fusion of the first 171 aa of the human HTT with 82 CAG and eGFP (hHTT-82Q-eGFP, CRISPR-HTT, n = 5, N = 2). As negative controls, cells were transfected only with plasmids encoding sgHTT1 and hHTT-82Q-eGFP (sgHTT1-only, n = 5, N = 2). Western blot with an antibody directed against eGFP, demonstrating the significantly lower levels of hHTT-82Q-eGFP protein in the CRISPR-HTT group than in sgHTT1-only samples, 7 days post-transfection.

(F) Western blots with an antibody recognizing the human HTT fragment demonstrated that mutant HTT levels were clearly lower in the CRISPR-HTT group than in the sgHTT1-only group, 4 weeks post-infection of primary neuronal cultures. Results are expressed as the mean ± SD. **p < 0.01, ***p < 0.001. Scale bar, 100 μm.

cells derived from human iPSCs (Figures 1D and 1E). The iPSCs were derived from a healthy subject and characterized as previously described (Figure S5) (Boissart et al., 2013). Briefly, we demonstrated the presence of pluripotent cells in iPSCs as well as the absence of chromosomal abnormalities. The neuronal cells derived from human iPSCs expressed the MAP2 and NeuN markers, and S100β was detected in immature glial cells and GFAP in astrocytes (Figure S5). Surveyor analysis and confocal acquisitions showed that eGFP had been edited in more than 30% of the cells, resulting in a strong loss of fluorescence in MAP2-positive neurons and S100β-positive glial cells (Figures 1D and 1E). The LV-CRISPR/Cas9 system therefore targeted genes very efficiently in both mouse and human neuronal or glial cells.

As an application of the CRISPR/Cas9 system to neurodegenerative disorders, we targeted the gene responsible for HD [for review, see Ross and Tabrizi (2011)]. We designed an sgRNA (sgHTT1) targeting a region close to the translation start site of the human *HTT* gene, with the aim of permanently blocking *HTT* expression (Figure 2A). Recently, studies demonstrated that non-allele selective *HTT* silencing in the adult brain is associated with improvements in HD pathology without deleterious effects (Boudreau et al., 2009; Drouet et al., 2009) and a phase I clinical trial is currently ongoing (Smith et al., 2016; Southwell et al., 2012). Although knockout studies showed that *HTT* is indispensable for embryonic development (Dragatsis et al., 1998; Saudou and Humbert, 2016; Zeitlin et al., 1995) and early conditional knockout leads to neuropathology (Dragatsis et al., 2000), or knockout on hemizygous background (Dietrich et al., 2017) leads to neuropathology, Wang et al. (2016) recently demonstrated that *HTT* ablation in adult neurons is non-deleterious. Furthermore long-term elimination of HTT in the cortex and striatum are well tolerated, supporting the design and evaluation of global *HTT* editing (mutant and wild-type alleles).

Transfection experiments in HEK293T cells showed that this sgRNA efficiently disrupted the endogenous human wild-type *HTT* gene (Figures 2A and 2B). Similarly, the sgHTT1 efficiently edited an exogenous human mutant *HTT* fragment fused to

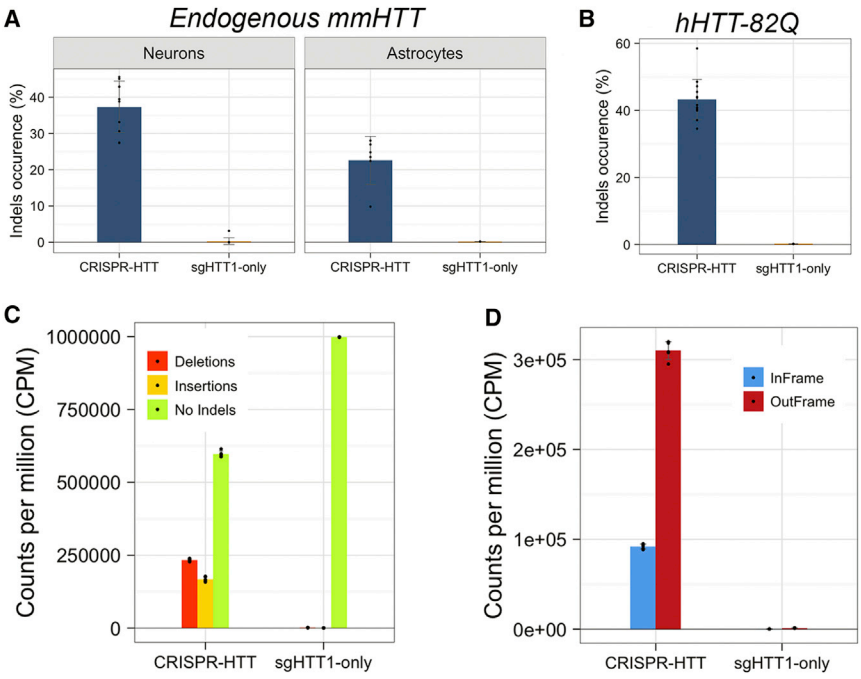

Figure 3. In Vitro *HTT* Editing in Primary Cultures of Mouse Cortical Neurons and Astrocytes

(A) Editing efficiency was evaluated for the endogenous mouse *HTT* (*mmHTT*) in primary cultures of neurons and astrocytes. Surveyor analysis revealed an efficient editing in the CRISPR-HTT group (neurons: n = 10, N = 2; astrocytes: n = 6, N = 1) compared to the controls (sgHTT1-only, neurons: n = 11, N = 2; astrocytes: n = 3, N = 1).

(B) Impact of hHTT-82Q editing in primary cultures of cortical neurons. Cortical neuronal cultures were infected with LV encoding Cas9, sgHTT1-mCherry, and hHTT-82Q (CRISPR-HTT, n = 6, N = 1). Cells infected with LV-sgHTT1-mCherry and LV-hHTT-82Q only were used as negative controls (sgHTT1-only, n = 6, N = 1). Surveyor assay demonstrates an efficient *hHTT-82Q* editing in the CRISPR-HTT group.

(C and D) The efficiency of *hHTT-82Q* editing in cultured neurons (CRISPR-HTT: n = 5; sgHTT1-only: n = 5) was evaluated by next-generation sequencing (NGS). Indels were highly frequent around the target site in the CRISPR-HTT group (C), with more than 75% of the indels detected resulting in frameshifts (D). Results are presented as mean ± SD. ***$p < 0.001$. Scale bar, 100 μm.

GFP (171 aa with 82 CAG repeats; hHTT82Q-eGFP), as indicated by the loss of GFP fluorescence (Figures 2C and 2D) and reduced GFP-HTT protein levels on western blot (Figure 2E). We previously showed that LV-mediated expression of an N-terminal fragment of mutant HTT in primary cultures faithfully reproduced gene expression changes seen in human HD, whereas control vectors have a minimal impact on transcriptional signature (Runne et al., 2008). Western blot analysis of samples treated with CRISPR-HTT revealed a drastic reduction of mutant HTT-82Q expression in primary cultures (Figure 2F). Surveyor analysis in primary cultures of cortical neurons and astrocytes indicates that endogenous mouse *HTT* gene (Figure 3A) is edited at similar efficiencies as the exogenous human *HTT-82Q* (Figure 3B), confirming the potential of sgHTT1 on diploid cells (Figure 3A). Next-generation sequencing (NGS) (MiSeq) analysis of on-target editing revealed that 40.2% of *HTT* reads contained deletions and insertions (indels) in the CRISPR-HTT group (Figure 3C; Tables S2 and S3), with 77.1% of the indels resulting in frameshifts (Figure 3D), in turn accounting for the lower level of mutant hHTT-82Q protein (Figure 2F).

We then used an HD model to assess the therapeutic benefits of disrupting the mutant human *HTT* gene. LV expressing the first 171 aa of the human *HTT* with 82 CAG repeats (hHTT-82Q) has been used to model HD in the mouse striatum (de Almeida et al., 2002). It caused a rapid accumulation of misfolded mutant HTT and key dysfunctions of striatal neurons related to HD, which were not observed in control groups expressing wild-type hHTT-18Q or eGFP. A large proportion of NGS reads (64%) containing indels and frameshifts were induced following NHEJ repair in 79.9% of the sequences (Figures 4D and 4E). The majority of reads containing indels displayed +1-bp insertion (>50%) and the remaining reads had mainly deletions, up to 17 bp (most often −1 and −3 bp, Tables S2 and S3). Finally, we showed that *hHTT-82Q* editing decreased aggregation of the mutant HTT protein (~36 aggregates/slice in CRISPR-HTT group versus ~171 aggregates/slice in sgHTT group) (Figures 4A and 4C) and preserved neuronal functions based on DARPP-32 expression; a marker of GABAergic neurons functionality that is decreased in HD (Figure 4B). These data demonstrate that the CRISPR system strongly disrupted the expression of a gene responsible for a disease in the CNS and prevented the appearance of typical HD pathological markers.

Precision and safety are prerequisites for the use of genome-editing tools in the study of brain disorders, and particularly for potential therapeutic applications. Long-term immune or inflammatory responses due to permanent expression of the bacterial Cas9 and off-target cleavage are key parameters of genome editing that must be checked and are mostly context and gene dependent (Dow et al., 2015). Blocking Cas9 expression after *HTT* editing might significantly improve the final outcome of the approach. We therefore designed a self-inactivating system called KamiCas9. For this, an additional sgRNA, expressed under the control of the weak 7SK promoter, targeted the ATG of Cas9 (sgCas9) in order to block its translation (Figure 5A). The co-transfection of HEK293T cells with plasmids encoding eGFP, Cas9, and sgGFP1/sgCas9 led to efficient disruption of the *Cas9* sequence (Figure S6B) and a decrease in Cas9 protein levels (Figure S6C), with no effect on *eGFP* editing efficiency (Figure S6B). We then evaluated the impact of Cas9 self-inactivation on *HTT* editing in the mouse striatum. Surveyor analysis demonstrated a very efficient disruption of *Cas9* gene (Figure 5B) and no difference between the constitutive CRISPR-HTT and KamiCas9-HTT on endogenous wild-type (WT) mouse *HTT* (mm*HTT*) (Figure 5B) and exogenous mutant *hHTT* editing efficiencies (Figure 5B). A second experiment was performed with a Cas9 nuclease containing a V5 tag in order to perform a

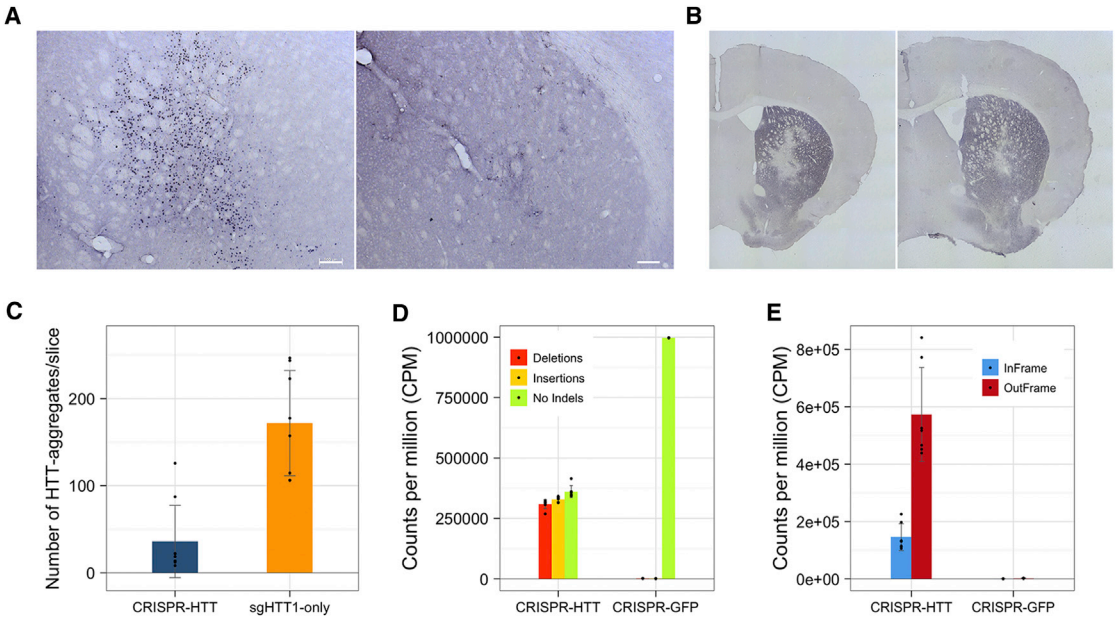

Figure 4. *HTT* Editing In Vivo

(A) Impact of mutant human HTT editing (hHTT-82Q) in vivo. LV encoding Cas9, sgHTT1-mCherry, and hHTT-82Q (CRISPR-HTT, n = 10) were co-injected in the striatum of WT mice. LV encoding Cas9, tdTomato-sgGFP1, and hHTT-82Q were used for the negative control group (CRISPR-GFP, n = 4). EM48 antibody staining revealed the accumulation of misfolded mutant hHTT-82Q in the control group (n = 8) and a drastic reduction in the CRISPR-HTT group (n = 10).

(B) DARPP-32 immunostaining showing the typical downregulation in the controls (n = 10) and a reduction of DARPP-32-negative area in the CRISPR-HTT group (n = 10).

(C) Quantification of HTT aggregates, showing lower levels of mutant HTT accumulation in the CRISPR-HTT group (n = 10) than in the negative controls (n = 8).

(D and E) The efficiency of hHTT-82Q editing (CRISPR-HTT: n = 7; sgHTT1-only: n = 3) was evaluated by NGS. Indels were highly frequent around the target site in the CRISPR-HTT group (D), with more than 75% of the indels detected resulting in frameshifts (E). Results are presented as mean ± SD. ***p < 0.001. Scale bar, 100 μm.

western blot analysis at 2 months (Figure 5C). A drastic reduction (>90%) of Cas9 protein was observed in KamiCas9-HTT-treated animals (Figure 5D). Finally, we tested the KamiCas9 system in 10- to 18-month-old knockin mice (Ki140CAG) (Menalled et al., 2003). Two months post-injection, indel frequencies were analyzed with the tracking of indels by decomposition (TIDE) method, which was developed for easy quantitative assessment of genome editing with sequence trace decomposition (Brinkman et al., 2014). We first validated that indel frequencies were similar with TIDE and MiSeq analysis (Figure 4; Figure S7). In the striatum of Ki140CAG mice, Cas9 editing reached 60.8% (Figure 5E). However, the percentage of indels was much lower for the *mmHTT* (2%–10%). This was associated with a slight reduction of mutant *mmHTT* aggregates (Figure 5F), but with no effect on rotarod motor behavior. The discrepancy between Cas9 and *mmHTT* editing was also observed in WT mice (Figure 5B) and is probably explained by the presence of a mismatch between the sgHTT1 and the mouse *HTT* sequence (Figure 3A), which are affecting in vivo *mmHTT* editing.

We therefore privileged the use of neurons derived from patient-specific iPSCs (HD-iPSCs with 60 CAG repeats) for the final validation and characterization of the KamiCas9-HTT system (Figure 6). To better reveal potential differences between the CRISPR and KamiCas9, we used suboptimal transduction conditions. One to 4 weeks later, DNA, RNA, and proteins were extracted from these cultures to measure the kinetics of sgRNA synthesis (Figure 6A), Cas9 and WT/mutant HTT indel frequencies (Figure 6B), and Cas9-V5 protein levels (Figure 6C). CRIPSR-GFP and KamiCas9-GFP were used as controls. Interestingly, the level of synthesis of sgHTT1 was much higher in the CRISPR-HTT/GFP vectors than in KamiCas9-HTT/GFP, probably due to promoter interference (Figure 6A). As expected, the weak 7SK promoter was leading to very low sgCas9 synthesis in the KamiCas9 system (10 times lower than H1-sgHTT1). Despite the low level of sgCas9 in KamiCas9 vectors, Cas9 indels progressively increased over time, from 15% at 1 week to 58% at 4 weeks (Figure 6B). A corresponding reduction of Cas9-V5 protein was measured by western blot (Figure 6C). TIDE analysis of the *HTT* gene editing confirmed that KamiCas9-HTT was as efficient as the constitutive CRISPR-HTT system (Figure 6B). We also showed that human WT and mutant endogenous *HTT* were edited at similar levels (Figure 6B). Four weeks post-infection, we re-challenged HD-iPS neurons with a LV-*HTT171-82Q* and measured residual editing activity 5 days later (Figure 6B). The *hHTT171-82Q* editing efficiency was undetectable in the Kamicas9-HTT group (Figure 6B), demonstrating the functional inactivation of the nuclease with KamiCas9 vectors.

Finally, we analyzed potential off-targets. Bioinformatic analysis identified 22 potential off-target (OT) sites in the human genome for sgHTT1, and 5 sites for sgCas9 (Figure 7A; Tables S4

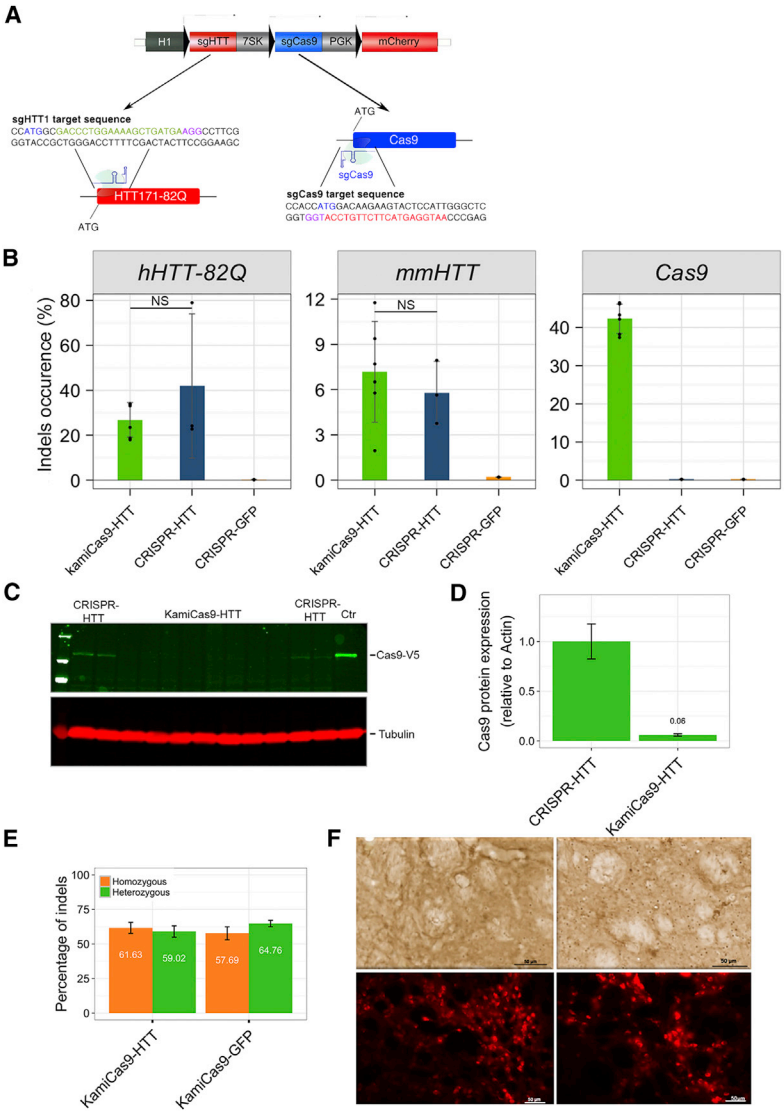

Figure 5. KamiCas9 Evaluation in WT and Ki140CAG Mice

(A) Schematic representation of the sgHTT1 and sgCas9 location in the human *HTT* and Cas9 genes and corresponding sequences. ATG: translational start sites.

(B) Cas9 was efficiently edited in the mouse brain (KamiCas9-HTT: n = 6; CRISPR-HTT, n = 3; CRISPR-GFP, n = 3) with no effect on the editing efficiency for the endogenous mouse *HTT* (*mmHTT*) or *hHTT-82Q*.

(C) Cas9-V5 protein level in the striatum of C57Bl/5 mice was significantly reduced 2 months post-injection of KamiCas9-HTT compared to CRISPR-HTT-treated mice (KamiCas9-HTT: n = 8; CRISPR-HTT, n = 4). As positive control, we used a protein extract from HEK293T cells transfected with the plasmid encoding Cas9-V5 nuclease.

(D) Quantitative analysis of the western blot.

(E) Cas9 editing measured by TIDE methods 2 months post-injection in the striatum of 10- to 18-month-old heterozygous and homozygous Ki140CAG mice [heterozygous KamiCas-HTT (n = 10), KamiCas9-GFP (n = 6); homozygous KamiCas9-HTT (n = 9), KamiCas9-GFP (n = 6)].

(F) Striatal sections from KamiCas9-GFP and KamiCas9-HTT animals. The impact on HTT aggregates was assessed with the EM48 anti-HTT antibody. Cherry-positive staining showing striatal neurons transduced with LV-KamiCas9-GFP and LV-KamiCas9-HTT. Scale bar, 50 μm.

See also Figure S5.

and S5). All of these sites contain at least two mismatches with the sgRNA (Figure 7B), and a few are located within the exons or introns of known genes (Figure 7C). Deep sequencing (MiSeq: Mapq > 25; mean reads per off-target, 27,500) of neurons derived from WT-iPSCs revealed undetectable off-target gene editing for 20/21 sgHTT (no PCR product for OT5; Figure 7D) and 5/5 sgCas9 sites (Figure 7E) as indicated by the equivalent levels of indels in controls and edited samples. The background levels differ between OT sites probably due to differences in PCR amplification and sequencing fidelity. Importantly, if double-strand breaks (DSBs) occur in 2.2% of the OT1 reads in CRISP-HTT samples, the inactivation of cas9 (KamiCas9) significantly reduced this frequency (79%; Figure 7D).

In conclusion, these collective results demonstrated the high on-target potency of KamiCas9 system in neuronal and glial cells of the mouse brain and in cultures derived from human HD-iPSCs. In addition, the molecular analyses demonstrated the improved safety profile of KamiCas9, which is essential in the context of CNS applications and in particular slowly progressive neurodegenerative diseases such as Huntington's disease.

DISCUSSION

We developed a highly efficient editing system for CNS applications. The potency of LV-KamiCas9 was demonstrated in mouse primary neuronal/glial cultures, in the striatum of mice, and in patient-specific iPSC neuronal derivatives. We showed that the kinetics of Cas9 expression shortly followed by self-inactivation provided high on-target editing while progressively inactivating the nuclease, therefore preventing further on- and off-target activities.

Several inducible systems based on chemical, optical, and transcriptional control of Cas9 RNA and protein levels have been described (Davis et al., 2015; Dow et al., 2015; Polstein and Gersbach, 2015; Zetsche et al., 2015). However, these strategies used complex systems or non-mammalian proteins, which might also induce a long-term inflammatory response (Favre et al., 2002). Our method has the advantage of requiring only the expression of an additional sgRNA and is therefore unlikely to have any long-term effects. This lentiviral-mediated in vivo delivery also provides attractive options for spCas9 in vivo genome editing due to its large transgene capacity. Finally, LV-KamiCas9 offers spatial and temporal control of gene editing in the CNS

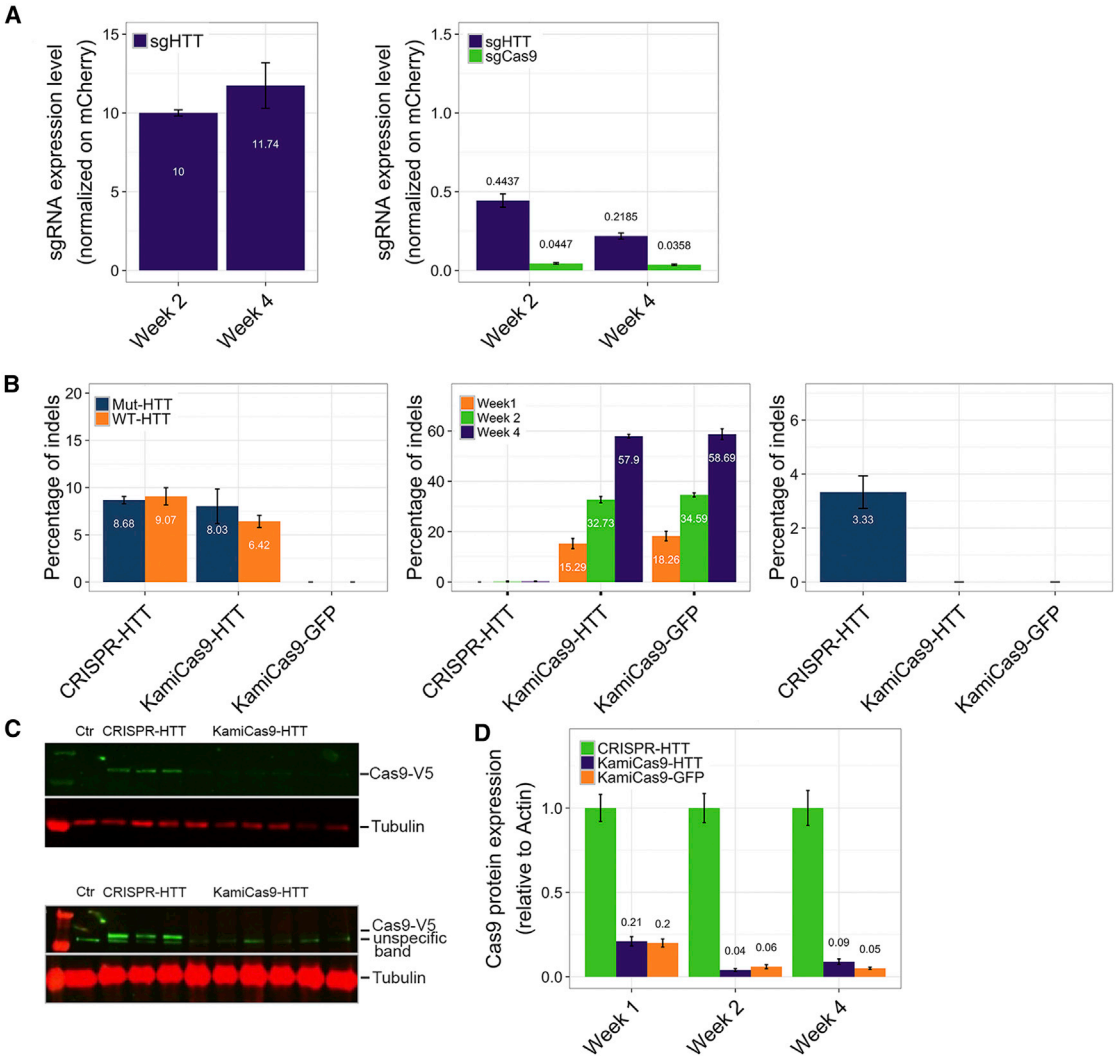

Figure 6. Kinetic of KamiCas9 Editing System in HD-iPSC-Derived Neurons

(A) Neurons derived from HD-iPSCs (60 CAG repeats) were infected with the KamiCas9-HTT and CRISPR-HTT systems. Two to 4 weeks later, the synthesis of the sgHTT1 and sgCas9 under the control of the H1 and 7SK promoters was measured by RT-qPCR. The level of sgHTT1 was higher in the CRISPR-HTT than in the KamiCas9-HTT. Similarly sgCas9 levels were ten times lower than the shHTT1 in the KamiCas9 system.

(B) Sequencing of PCR products corresponding to human WT and mutant HTT revealed similar editing efficiencies. A progressive increase in Cas9 editing was observed over time, reaching 58% at 4 weeks. At 4 weeks, we challenged the system with a LV-Htt171-82Q, and 5 days later we specifically measured the editing of the mutant HTT171-82Q. This demonstrated that Cas9 self-inactivation was sufficient to prevent detectable editing.

(C) Western blot analysis showing the decrease of Cas-V5 protein at 4 weeks in the KamiCas9 samples.

(D) Quantitative analysis of Cas9 western blot at 1, 2, and 4 weeks post-infection.

with opportunities to modulate tropism and cell-type specificities (Colin et al., 2009) as well as to integrate brain circuitry information to reach large brain areas with local intraparenchymal administrations (Hirano et al., 2013).

This KamiCas9 self-inactivating editing system was used to inactivate a prototypical disease gene of the CNS, the *HTT* gene (Kolli et al., 2017; Monteys et al., 2017; Shin et al., 2016; Yang et al., 2017). These studies demonstrated an efficient disruption of an exogenous/endogenous WT/mutant *HTT* gene associated with a decreased HTT aggregation, as well as reduced neuronal dysfunction both in vitro and in vivo. In the present study, we applied and characterized *HTT* gene editing in HD-iPSC neuronal derivatives, which closely reproduce molecular and cellular features of HD (An et al., 2014; Ross and Akimov, 2014). Experiments in this model are particularly valuable not only to assess efficacy and safety concerns but also to demonstrate the rescue of mutant HTT phenotype following editing. Additional studies are, however, warranted to evaluate the consequence of non-allele selective *HTT* disruption with the CRISPR/Cas9 system. Studies at the cellular level should provide data on mono- and bi-allelic editing frequencies and consequences on cellular WT/mutant *HTT* expression levels. These

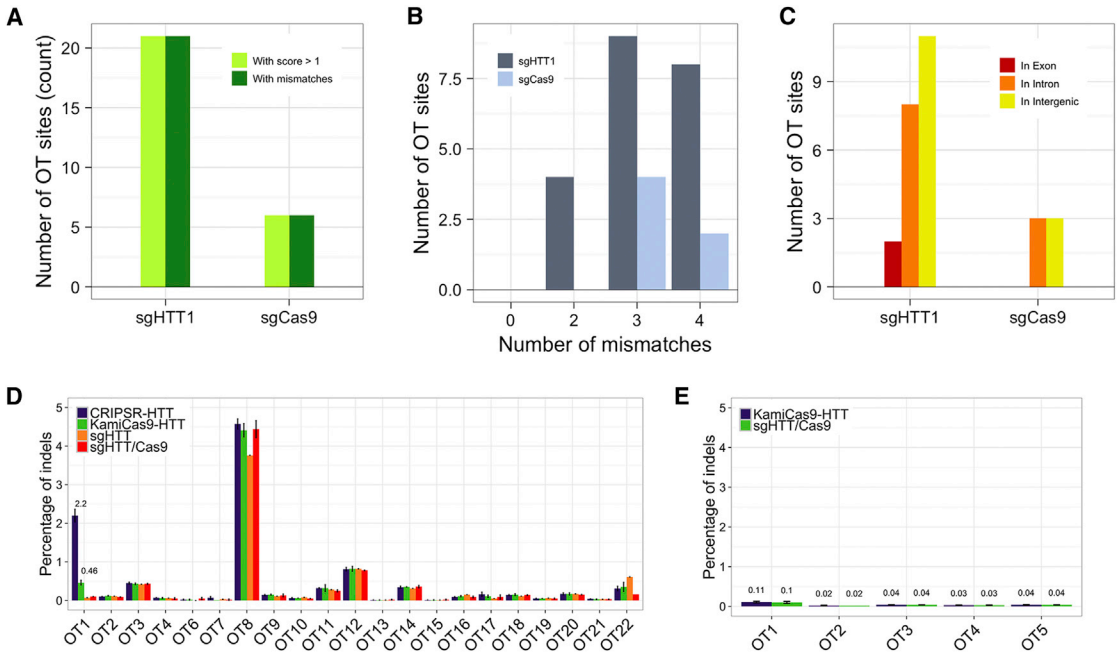

Figure 7. Off-Target Analysis

(A and B) Bioinformatic analysis revealed potential off-target sites for sgHTT1 and sgCas9 (A), with at least two mismatches between the off-target sequence and the sgRNA in each case (B).

(C) A few of these off-target sites were located in known protein-coding genes (exons or introns).

(D) sgHTT off-target analysis by NGS sequencing in neurons derived from WT-iPSCs. Differentiated neurons were infected with KamiCas9-HTT (n = 3), sgHTT/sgCas9 (n = 2), CRISPR-HTT (n = 3), and sgHTT (n = 1). Three weeks post-infection, the DNA was extracted and the PCR products of the potential off-target sites were analyzed by sequencing to determine the percentage of genome editing.

(E) The analysis of sgCas9 off-target sites revealed undetectable cleavage. OT, off-target.

HD-iPSCs will provide an opportunity to decipher the contribution of cell-type-specific *HTT* functions and cellular pathways implicated in HD in complex heterogeneous cultures. The partial knockdown of mutant *HTT* expression by RNA silencing has been shown to be sufficient to slow the progression of neuronal dysfunction and death in various animal models of HD, and a clinical trial based on this approach is currently underway (Smith et al., 2016) (Roche Isis Pharmaceuticals; https://en.hdbuzz.net/182). Genome editing has the advantage of being able to block *HTT* expression in a complete and permanent manner. In addition, ATG-independent HTT translation (RAN translation) has been observed in HD patients and can induce the accumulation of other expanded species (Bañez-Coronel et al, 2015). Frameshifts before the CAG expansion can lead to an early STOP codon avoiding the synthesis of the CAG expanded track but can also modify the reading frame to synthetize other expanded sequences. In our study, analysis of sequencing reads demonstrated that the majority of edited *HTT* alleles have either an early STOP codon before the CAG or can induce the synthesis of an expanded alanine-containing HTT, which has not been associated with any sign of toxicity with classical CAG length observed in HD. The therapeutic benefits observed in our models support the absence of toxic RAN translation following *HTT* ATG editing.

LV-KamiCas9-HTT is efficiently targeting the *HTT* loci within the genome. However, cleavages at sites with sequences homologies with sgHTT1 and sgCas9 might occur, and the frequency of OT activities is sgRNA sequence dependent. To test whether Kamicas9-HTT exhibits reduced off-target effects in human cells, we performed high-throughput sequencing of all OT sites with two to four predicted mismatches in the reference human genome. The sequencing data showed that sgCas9 did not yield any detectable off-target cleavages, supporting the use of this sgCas9 for all KamiCas9 applications. Twenty of the 21 OT sites were statistically indistinguishable from the background level observed in control conditions, therefore demonstrating a complete absence of off-target events for most sites. In OT1, a low editing activity was detected in CRISPR-HTT samples, but a transient expression of the Cas9 nuclease, with the KamiCas9-HTT, nearly completely abrogated this off-target activity. The use of high-fidelity Cas9 might further improve the biosafety of the system (Kleinstiver et al., 2016; Slaymaker et al., 2016).

These data highlight the considerable potential of this strategy for treating genetic disorders of the brain. The high editing efficiency achieved in this study raises the possibility of using similar experimental strategies for other monogenic brain diseases. In addition, the ability of the CRISPR/Cas9 system to target multiple genes simultaneously makes it a powerful tool for modeling complex sporadic diseases developing at the interface between genetic risk factors and a specific environment. We are confident that this study will pave the way for further improvements of CRISPR/Cas9 technology and its use in the adult brain to decipher the key mechanisms underlying neurodegenerative

diseases and for the development of therapeutic approaches based on gene editing.

EXPERIMENTAL PROCEDURES

Further details and an outline of resources used in this work can be found in Supplemental Experimental Procedures.

Animal Experiments

Male and female 10-week-old (adult) C57BL/6 (Janvier, Le Genest-Saint-Isle, France) and BAC-GLT1-eGFP transgenic mice expressing eGFP specifically in astrocytes (kindly provided by Prof. J. Rothstein, Baltimore, MD) (Regan et al., 2007) were used for in vivo experiments. Pregnant FvB mice were used for primary culture experiments (Janvier, Le Genest-Saint-Isle, France). Mice were housed in a specific pathogen-free (SPF) facility with IVC cages GM500 (Tecniplast) or rat R.BTM.U × /R.ICV.6 cages (Innovive) and Innorack rats, simple face (catalog #RS.5.8.40) containing corn cob bedding with five mice per cage maximum. The animals were maintained in a controlled-temperature room (22 ± 1°C) and under a 14-hr light/10-hr dark cycle. Breeding program is dependent of strains or productivity requests but are regularly trio or couple breeders. Enrichments are two pieces of wipes, one cardboard tunnel, one cardboard or polysulfone house with two entrances/exits. Food [global rodent diet XP-18, vitamin-fortified, irradiated at 25 kGy (Kliba Nafag AG, Kaiseraugst, Switzerland; catalog #3242)] and water were provided ad libitum. All experimental procedures were performed in strict accordance with Swiss regulations concerning the care and use of laboratory animals (veterinary authorizations: 2782, 2888, and 3073). During the surgery, body temperature was controlled with a warming blanket (CMA 450 Temperature Controller; Phymep, Paris, France), and the eyes were protected with 0.2% Viscotears liquid gel (Novartis, Basel, Switzerland). Post-surgery analgesic treatment was administered for 72 hr with paracetamol (Dafalgan Upsa; 1,000 mg/750 mL) in the drinking water.

Ki140CAG Mice

In the present study, we used knockin mice expressing chimeric mouse/human exon 1 containing 140 CAG repeats inserted in the murine *HTT* gene (Ki140CAG). The Ki140CAG mice colony was maintained by breeding heterozygotes Ki140CAG males and females (Menalled et al., 2003). Mice were N3 (B6) on a 129 Sv × C57BL/6J background. The characteristics of the animals in each group are indicated in Table S1. Littermates were used as controls. The environment was enriched with a piece of absorbent paper. Breeder animals also received red mouse houses. The temperature of the housed room was controlled and maintained on a 12-hr light/dark cycle. Food and water were available ad libitum. All animal studies were conducted according to the French regulation (EU Directive 2010/63/EU—French Act Rural Code R 214-87 to 131). The animal facility was approved by veterinarian inspectors (authorization no. A 92-032-02) and complies with Standards for Humane Care and Use of Laboratory Animals of the Office of Laboratory Animal Welfare (OLAW) (no. A5826-01). All procedures received approval from the ethical committee [authorization no. 2015060417243726vl (APAFIS#770)]. Genotype was determined from PCR of tail snips taken at 21 days of age.

In these studies, only animals with technical failures (for example, problems with the injection or surgery) were excluded. Animal sample size was determined based on previous studies using related experimental procedures to allow robust statistical analyzes and reproducibility (Drouet et al., 2009, 2014). No randomization was used to allocate animals to experimental groups. No specific order was used to treat the animals. Each in vivo experiment was replicated ones.

Human iPSCs

Reprogramming, Culture of iPSCs

All experiments on human samples were performed in accordance with the requirements of the Swiss ethics committee (approved protocol 107/13_3). Human iPSCs were derived from peripheral blood mononuclear cells (PBMCs) from a healthy subject, based on previous publications (Boissart et al., 2013; Lee et al., 2015). iPSCs were routinely cultured and their quality was checked (morphology, alkaline phosphatase staining, embryonic body differentiation, staining, and karyotyping), as previously described (Boissart et al., 2013; Lee et al., 2015). The human HD-iPSC line (60 CAG HD line) from Coriell Institute for Medical Research is cultured on L7 (Lonza) matrix in STEMPRO medium (Invitrogen) supplemented with 10 ng/mL recombinant human FGF2. Cells are fed daily and manually passaged every 5–7 days. Human striatal neuronal cultures with HD mutation were produced as previously described (Arber et al., 2015; Nicoleau et al., 2013).

Differentiation, Culture of Human Neurons and Glial Cells

iPSCs from passage 20 were used for neural stem cell (NSC) differentiation, as previously described (Boissart et al., 2013). The NSC medium was changed every 2 days and cells were passaged once per week, as previously described (Boissart et al., 2013). The NSCs were amplified, frozen, and stored in liquid nitrogen until use. NSCs between passages 9 and 12 were used for differentiation into neurons and glial cells. Briefly, the NSC medium was removed and cells were incubated in 500 μL of trypsin (Gibco, Life Technologies, Zug, Switzerland) at 37°C for 3–5 min, to detach them from the plate. Trypsin activity was inhibited by the direct addition of 10% FBS to the plate, and the detached cells were transferred to a Falcon tube containing 4.5 mL of N2B27 medium (N2B27: 1:1 Neurobasal:DMEM-F12-Glutamax, 2% B27, 1% N2, 0.1% gentamicin; Gibco, Life Technologies, Zug, Switzerland). Cells were centrifuged at 300 × *g* for 5 min at room temperature. The supernatant was removed, and the cells were resuspended in 1 mL of N2B27. NSCs were counted in a hemocytometer. For differentiation into a coculture of neuronal/glial cells, we plated NSCs at a density of 50,000 NSCs/cm^2 in 500 μL of medium in the wells of a 24-well plate, each well containing a glass coverslip coated with 1/6 poly-ornithine (Sigma-Aldrich, Buchs, Switzerland) for 24 hr and then with 2 μg/mL laminin (Sigma-Aldrich, Buchs, Switzerland) for 24 hr. The appropriate number of NSCs were thus transferred to a neuronal culture medium consisting of Neurobasal (Gibco, Life Technologies, Zug, Switzerland), 2% B27 (Gibco, Life Technologies, Zug, Switzerland), 1% Glutamax (Gibco, Life Technologies, Zug, Switzerland), 0.1% gentamicin (Gibco, Life Technologies, Zug, Switzerland), 20 ng/mL BDNF (Miltenyi Biotech, Bergisch-Gladbach, Germany), 25 ng/mL activin A (R&D Systems Europe, Bio-techne AG, Zug, Switzerland), and 2 μg/mL laminin (Sigma-Aldrich, Buchs, Switzerland). The medium was completely replaced every 3 days, and cultures were maintained for up to 6 weeks.

Culture of Human HD-NSCs

Human HD-NSCs were maintained as immature and cultured as previously described. The NSC medium, composed of N2B27 medium with 20 ng/mL BDNF (Miltenyi Biotech, Bergisch-Gladbach, Germany), 10 ng/mL epidermal growth factor (EGF) (REF), and 10 ng/mL basic fibroblast growth factor (bFGF) (REF), was changed every 2 days. Cells were passaged once per week, at a density of 100,000 NSCs/cm^2 in 500 μL of medium in the wells of a six-well plate, coated with 1/6 poly-ornithine (Sigma-Aldrich, Buchs, Switzerland) for 24 hr and then with 2 μg/mL laminin (Sigma-Aldrich, Buchs, Switzerland) for 24 hr.

Statistical Methods

For the statistical analyses, normality of the distribution and equality of the variances were assessed to determine the type of statistical tests. For two-groups comparison, Student's t test was performed with Excel software. For comparisons larger than two groups, ANOVA and post hoc analyses were performed with the Statistica software. Predictive bioinformatic analyses to detect potential off-target sites in the human genome were performed with the CRISPRseek package with R software. For all experiments, groups of samples were used for statistical analyzes. Statistical tests were defined as significant if the probability of null hypothesis acceptance was below 5%. No specific method was used for sample randomization, sample size estimation, or inclusion/exclusion of data. Results are presented as the mean ± SD. *$p < 0.05$, **$p < 0.01$, and ***$p < 0.001$.

ACCESSION NUMBERS

The accession number for the RNA-seq data reported in this study is NCBI Bioproject: PRJNA395854.

SUPPLEMENTAL INFORMATION

Supplemental Information includes Supplemental Experimental Procedures, seven figures, and five tables and can be found with this article online at http://dx.doi.org/10.1016/j.celrep.2017.08.075.

AUTHOR CONTRIBUTIONS

N.D., N.M., G.V., and A.P. conceived the experiments. N.M. and G.V. performed the experiments. L.d.L., E.B., C.M., L.H., T.B., A.P., and T.D. participated in some of the experiments. N.M., G.V., C.M., V.Z., G.P., A. Maulet, and M.C. performed routine cultures of iPSCs and NSCs. N.M., A. Maulet, and C.M. optimized and cultured human neurons. N.M., G.V., and C.M. developed the bioinformatics pipeline and performed the on- and off-target analysis by NGS. M.R., C.P., and A. Mathias provided technical support for cell cultures and viral vector production. N.D., N.M., and G.V. wrote the article. R.d.P. and L.P. provided expertise and feedback. All authors edited the manuscript.

ACKNOWLEDGMENTS

We would like to thank Dr. Jean-Yves Chatton and the Cellular Imaging Facility (CIF) (University of Lausanne) for valuable advice concerning microscopy. We thank Dr. Keith Harshman and the Lausanne Genomic Technologies Facility (University of Lausanne) for NGS. We thank Dr. S. Zeitlin, Dr. M. Levine, and Dr. S. Humbert for their help in getting the breeders for starting our Ki140CAG mouse colony. We thank Prof. Micah Murray for the language and grammar corrections. This work was supported by grants from the Swiss National Science Foundation (31003A-165834), Association Française contre les Myopathies (AFM-Téléthon), the Agence Nationale pour la Recherche, Neuratris (Grant Q5 "Investment for the Future"; ANR-11-INBS-0011), Laboratoire d'Excellence Revive (Investissement d'Avenir; ANR-10-LABX-73), the French National Health Institute (INSERM), the Novartis Foundation, and the EU Joint Programme–Neurodegenerative Disease Research (JPND) Project (Grant Agreement No. 643417). This specific part of the project is supported through the following organizations under the aegis of JPND (http://www.neurodegenerationresearch.eu/) (France, French National Research Agency [ANR], Switzerland, State Secretariat for Education, Research, and Innovation [SERI], and the Swiss National Science Foundation FN 31ND30-166947/1). N.M. and N.D. are co-inventors on a patent application filed by Lausanne University Hospital and relating to CRISPR (WO 2016/020399 A1, PCT/EP2015/067986). The plasmid containing the GfaABC1D promoter is available under a material transfer agreement (MTA) from Dr. Brenner (Birmingham, AL). L.d.L. is recipient of a PhD fellowship from the Fondation pour la Recherche Médicale.

Received: August 16, 2016
Revised: July 14, 2017
Accepted: August 23, 2017
Published: September 19, 2017

REFERENCES

An, M.C., O'Brien, R.N., Zhang, N., Patra, B.N., De La Cruz, M., Ray, A., and Ellerby, L.M. (2014). Polyglutamine disease modeling: epitope based screen for homologous recombination using CRISPR/Cas9 system. PLoS Curr. *6*, ecurrents.hd.0242d2e7ad72225efa72f6964589369a.

Arber, C., Precious, S.V., Cambray, S., Risner-Janiczek, J.R., Kelly, C., Noakes, Z., Fjodorova, M., Heuer, A., Ungless, M.A., Rodriguez, T.A., et al. (2015). Activin A directs striatal projection neuron differentiation of human pluripotent stem cells. Development *142*, 1375–1386.

Bañez-Coronel, M., Ayhan, F., Tarabochia, A.D., Zu, T., Perez, B.A., Tusi, S.K., Pletnikova, O., Borchelt, D.R., Ross, C.A., Margolis, R.L., et al. (2015). RAN translation in huntington disease. Neuron *88*, 667–677.

Bates, G.P., Dorsey, R., Gusella, J.F., Hayden, M.R., Kay, C., Leavitt, B.R., Nance, M., Ross, C.A., Scahill, R.I., Wetzel, R., et al. (2015). Huntington disease. Nat. Rev. Dis. Primers *1*, 15005.

Bibb, J.A., Yan, Z., Svenningsson, P., Snyder, G.L., Pieribone, V.A., Horiuchi, A., Nairn, A.C., Messer, A., and Greengard, P. (2000). Severe deficiencies in dopamine signaling in presymptomatic Huntington's disease mice. Proc. Natl. Acad. Sci. USA *97*, 6809–6814.

Boissart, C., Poulet, A., Georges, P., Darville, H., Julita, E., Delorme, R., Bourgeron, T., Peschanski, M., and Benchoua, A. (2013). Differentiation from human pluripotent stem cells of cortical neurons of the superficial layers amenable to psychiatric disease modeling and high-throughput drug screening. Transl. Psychiatry *3*, e294.

Boudreau, R.L., McBride, J.L., Martins, I., Shen, S., Xing, Y., Carter, B.J., and Davidson, B.L. (2009). Nonallele-specific silencing of mutant and wild-type huntingtin demonstrates therapeutic efficacy in Huntington's disease mice. Mol. Ther. *17*, 1053–1063.

Brinkman, E.K., Chen, T., Amendola, M., and van Steensel, B. (2014). Easy quantitative assessment of genome editing by sequence trace decomposition. Nucleic Acids Res. *42*, e168.

Cambon, K., Zimmer, V., Martineau, S., Gaillard, M.C., Jarrige, M., Bugi, A., Miniarikova, J., Rey, M., Hassig, R., Dufour, N., et al. (2017). Preclinical evaluation of a lentiviral vector for Huntingtin silencing. Mol. Ther. Methods Clin. Dev. *5*, 259–276.

Cartier, N., Hacein-Bey-Abina, S., Bartholomae, C.C., Veres, G., Schmidt, M., Kutschera, I., Vidaud, M., Abel, U., Dal-Cortivo, L., Caccavelli, L., et al. (2009). Hematopoietic stem cell gene therapy with a lentiviral vector in X-linked adrenoleukodystrophy. Science *326*, 818–823.

Colin, A., Faideau, M., Dufour, N., Auregan, G., Hassig, R., Andrieu, T., Brouillet, E., Hantraye, P., Bonvento, G., and Déglon, N. (2009). Engineered lentiviral vector targeting astrocytes in vivo. Glia *57*, 667–679.

Cong, L., Ran, F.A., Cox, D., Lin, S., Barretto, R., Habib, N., Hsu, P.D., Wu, X., Jiang, W., Marraffini, L.A., and Zhang, F. (2013). Multiplex genome engineering using CRISPR/Cas systems. Science *339*, 819–823.

Davis, K.M., Pattanayak, V., Thompson, D.B., Zuris, J.A., and Liu, D.R. (2015). Small molecule-triggered Cas9 protein with improved genome-editing specificity. Nat. Chem. Biol. *11*, 316–318.

de Almeida, L.P., Ross, C.A., Zala, D., Aebischer, P., and Déglon, N. (2002). Lentiviral-mediated delivery of mutant huntingtin in the striatum of rats induces a selective neuropathology modulated by polyglutamine repeat size, huntingtin expression levels, and protein length. J. Neurosci. *22*, 3473–3483.

de Leeuw, B., Su, M., ter Horst, M., Iwata, S., Rodijk, M., Hoeben, R.C., Messing, A., Smitt, P.S., and Brenner, M. (2006). Increased glia-specific transgene expression with glial fibrillary acidic protein promoters containing multiple enhancer elements. J. Neurosci. Res. *83*, 744–753.

Déglon, N., Tseng, J.L., Bensadoun, J.C., Zurn, A.D., Arsenijevic, Y., Pereira de Almeida, L., Zufferey, R., Trono, D., and Aebischer, P. (2000). Self-inactivating lentiviral vectors with enhanced transgene expression as potential gene transfer system in Parkinson's disease. Hum. Gene Ther. *11*, 179–190.

Dietrich, P., Johnson, I.M., Alli, S., and Dragatsis, I. (2017). Elimination of huntingtin in the adult mouse leads to progressive behavioral deficits, bilateral thalamic calcification, and altered brain iron homeostasis. PLoS Genet. *13*, e1006846.

Dow, L.E., Fisher, J., O'Rourke, K.P., Muley, A., Kastenhuber, E.R., Livshits, G., Tschaharganeh, D.F., Socci, N.D., and Lowe, S.W. (2015). Inducible in vivo genome editing with CRISPR-Cas9. Nat. Biotechnol. *33*, 390–394.

Dragatsis, I., Efstratiadis, A., and Zeitlin, S. (1998). Mouse mutant embryos lacking huntingtin are rescued from lethality by wild-type extraembryonic tissues. Development *125*, 1529–1539.

Dragatsis, I., Levine, M.S., and Zeitlin, S. (2000). Inactivation of Hdh in the brain and testis results in progressive neurodegeneration and sterility in mice. Nat. Genet. *26*, 300–306.

Drouet, V., Perrin, V., Hassig, R., Dufour, N., Auregan, G., Alves, S., Bonvento, G., Brouillet, E., Luthi-Carter, R., Hantraye, P., and Déglon, N. (2009). Sustained effects of nonallele-specific Huntingtin silencing. Ann. Neurol. *65*, 276–285.

Drouet, V., Ruiz, M., Zala, D., Feyeux, M., Auregan, G., Cambon, K., Troquier, L., Carpentier, J., Aubert, S., Merienne, N., et al. (2014). Allele-specific silencing of mutant huntingtin in rodent brain and human stem cells. PLoS One *9*, e99341.

Favre, D., Blouin, V., Provost, N., Spisek, R., Porrot, F., Bohl, D., Marmé, F., Chérel, Y., Salvetti, A., Hurtrel, B., et al. (2002). Lack of an immune response against the tetracycline-dependent transactivator correlates with long-term doxycycline-regulated transgene expression in nonhuman primates after intramuscular injection of recombinant adeno-associated virus. J. Virol. *76*, 11605–11611.

Hirano, M., Kato, S., Kobayashi, K., Okada, T., Yaginuma, H., and Kobayashi, K. (2013). Highly efficient retrograde gene transfer into motor neurons by a lentiviral vector pseudotyped with fusion glycoprotein. PLoS One *8*, e75896.

Izpisua Belmonte, J.C., Callaway, E.M., Caddick, S.J., Churchland, P., Feng, G., Homanics, G.E., Lee, K.F., Leopold, D.A., Miller, C.T., Mitchell, J.F., et al. (2015). Brains, genes, and primates. Neuron *86*, 617–631.

Jarraya, B., Boulet, S., Ralph, G.S., Jan, C., Bonvento, G., Azzouz, M., Miskin, J.E., Shin, M., Delzescaux, T., Drouot, X., et al. (2009). Dopamine gene therapy for Parkinson's disease in a nonhuman primate without associated dyskinesia. Sci. Transl. Med. *1*, 2ra4.

Kleinstiver, B.P., Pattanayak, V., Prew, M.S., Tsai, S.Q., Nguyen, N.T., Zheng, Z., and Joung, J.K. (2016). High-fidelity CRISPR-Cas9 nucleases with no detectable genome-wide off-target effects. Nature *529*, 490–495.

Kolli, N., Lu, M., Maiti, P., Rossignol, J., and Dunbar, G.L. (2017). CRISPR-Cas9 mediated gene-silencing of the mutant huntingtin gene in an in vitro model of Huntington's disease. Int. J. Mol. Sci. *18*, 754.

Lee, H.K., Morin, P., Wells, J., Hanlon, E.B., and Xia, W. (2015). Induced pluripotent stem cells (iPSCs) derived from frontotemporal dementia patient's peripheral blood mononuclear cells. Stem Cell Res. *15*, 325–327.

Long, C., Amoasii, L., Mireault, A.A., McAnally, J.R., Li, H., Sanchez-Ortiz, E., Bhattacharyya, S., Shelton, J.M., Bassel-Duby, R., and Olson, E.N. (2016). Postnatal genome editing partially restores dystrophin expression in a mouse model of muscular dystrophy. Science *351*, 400–403.

Luthi-Carter, R., Strand, A., Peters, N.L., Solano, S.M., Hollingsworth, Z.R., Menon, A.S., Frey, A.S., Spektor, B.S., Penney, E.B., Schilling, G., et al. (2000). Decreased expression of striatal signaling genes in a mouse model of Huntington's disease. Hum. Mol. Genet. *9*, 1259–1271.

Mali, P., Yang, L., Esvelt, K.M., Aach, J., Guell, M., DiCarlo, J.E., Norville, J.E., and Church, G.M. (2013). RNA-guided human genome engineering via Cas9. Science *339*, 823–826.

Menalled, L.B., Sison, J.D., Dragatsis, I., Zeitlin, S., and Chesselet, M.F. (2003). Time course of early motor and neuropathological anomalies in a knock-in mouse model of Huntington's disease with 140 CAG repeats. J. Comp. Neurol. *465*, 11–26.

Merienne, N., Le Douce, J., Faivre, E., Déglon, N., and Bonvento, G. (2013). Efficient gene delivery and selective transduction of astrocytes in the mammalian brain using viral vectors. Front. Cell. Neurosci. *7*, 106.

Monteys, A.M., Ebanks, S.A., Keiser, M.S., and Davidson, B.L. (2017). CRISPR/Cas9 editing of the mutant Huntingtin allele in vitro and in vivo. Mol. Ther. *25*, 12–23.

Naldini, L., Blömer, U., Gallay, P., Ory, D., Mulligan, R., Gage, F.H., Verma, I.M., and Trono, D. (1996). In vivo gene delivery and stable transduction of nondividing cells by a lentiviral vector. Science *272*, 263–267.

Nelson, C.E., Hakim, C.H., Ousterout, D.G., Thakore, P.I., Moreb, E.A., Castellanos Rivera, R.M., Madhavan, S., Pan, X., Ran, F.A., Yan, W.X., et al. (2016). In vivo genome editing improves muscle function in a mouse model of Duchenne muscular dystrophy. Science *351*, 403–407.

Nicoleau, C., Varela, C., Bonnefond, C., Maury, Y., Bugi, A., Aubry, L., Viegas, P., Bourgois-Rocha, F., Peschanski, M., and Perrier, A.L. (2013). Embryonic stem cells neural differentiation qualifies the role of Wnt/beta-Catenin signals in human telencephalic specification and regionalization. Stem Cells *31*, 1763–1774.

Ouimet, C.C., Langley-Gullion, K.C., and Greengard, P. (1998). Quantitative immunocytochemistry of DARPP-32-expressing neurons in the rat caudatoputamen. Brain Res. *808*, 8–12.

Polstein, L.R., and Gersbach, C.A. (2015). A light-inducible CRISPR-Cas9 system for control of endogenous gene activation. Nat. Chem. Biol. *11*, 198–200.

Regan, M.R., Huang, Y.H., Kim, Y.S., Dykes-Hoberg, M.I., Jin, L., Watkins, A.M., Bergles, D.E., and Rothstein, J.D. (2007). Variations in promoter activity reveal a differential expression and physiology of glutamate transporters by glia in the developing and mature CNS. J Neurosci. *27*, 6607–6619.

Ross, C.A., and Akimov, S.S. (2014). Human-induced pluripotent stem cells: potential for neurodegenerative diseases. Hum. Mol. Genet. *23* (*R1*), R17–R26.

Ross, C.A., and Tabrizi, S.J. (2011). Huntington's disease: from molecular pathogenesis to clinical treatment. Lancet Neurol. *10*, 83–98.

Runne, H., Régulier, E., Kuhn, A., Zala, D., Gokce, O., Perrin, V., Sick, B., Aebischer, P., Déglon, N., and Luthi-Carter, R. (2008). Dysregulation of gene expression in primary neuron models of Huntington's disease shows that polyglutamine-related effects on the striatal transcriptome may not be dependent on brain circuitry. J. Neurosci. *28*, 9723–9731.

Saudou, F., and Humbert, S. (2016). The biology of Huntingtin. Neuron *89*, 910–926.

Shalem, O., Sanjana, N.E., and Zhang, F. (2015). High-throughput functional genomics using CRISPR-Cas9. Nat. Rev. Genet. *16*, 299–311.

Shin, J.W., Kim, K.H., Chao, M.J., Atwal, R.S., Gillis, T., MacDonald, M.E., Gusella, J.F., and Lee, J.M. (2016). Permanent inactivation of Huntington's disease mutation by personalized allele-specific CRISPR/Cas9. Hum. Mol. Genet. *25*, 4566–4576.

Shin, A., Shin, B., Shin, J.W., Kim, K.H., Atwal, R.S., Hope, J.M., Gillis, T., Leszyk, J.D., Shaffer, S.A., Lee, R., et al. (2017). Novel allele-specific quantification methods reveal no effects of adult onset CAG repeats on HTT mRNA and protein levels. Hum. Mol. Genet. *26*, 1258–1267.

Slaymaker, I.M., Gao, L., Zetsche, B., Scott, D.A., Yan, W.X., and Zhang, F. (2016). Rationally engineered Cas9 nucleases with improved specificity. Science *351*, 84–88.

Smith, A., Zanardi, T., Norris, D., Swayze, E., Baumann, T., Bowyer, K., Hung, G., and Mendoza, J. (2016). Antisense oligonucleotides enter clinical trials. HD Insights *13*, 10–15.

Southwell, A.L., Skotte, N.H., Bennett, C.F., and Hayden, M.R. (2012). Antisense oligonucleotide therapeutics for inherited neurodegenerative diseases. Trends Mol. Med. *18*, 634–643.

Swiech, L., Heidenreich, M., Banerjee, A., Habib, N., Li, Y., Trombetta, J., Sur, M., and Zhang, F. (2015). In vivo interrogation of gene function in the mammalian brain using CRISPR-Cas9. Nat. Biotechnol. *33*, 102–106.

Tabebordbar, M., Zhu, K., Cheng, J.K.W., Chew, W.L., Widrick, J.J., Yan, W.X., Maesner, C., Wu, E.Y., Xiao, R., Ran, F.A., et al. (2016). In vivo gene editing in dystrophic mouse muscle and muscle stem cells. Science *351*, 407–411.

van Dellen, A., Welch, J., Dixon, R.M., Cordery, P., York, D., Styles, P., Blakemore, C., and Hannan, A.J. (2000). *N*-Acetylaspartate and DARPP-32 levels decrease in the corpus striatum of Huntington's disease mice. Neuroreport *11*, 3751–3757.

Wang, G., Liu, X., Gaertig, M.A., Li, S., and Li, X.J. (2016). Ablation of huntingtin in adult neurons is nondeleterious but its depletion in young mice causes acute pancreatitis. Proc. Natl. Acad. Sci. USA *113*, 3359–3364.

Wu, Y.T., Fratiglioni, L., Matthews, F.E., Lobo, A., Breteler, M.M., Skoog, I., and Brayne, C. (2016). Dementia in western Europe: epidemiological evidence and implications for policy making. Lancet Neurol. *15*, 116–124.

Yang, W., Tu, Z., Sun, Q., and Li, X.J. (2016). CRISPR/Cas9: implications for modeling and therapy of neurodegenerative diseases. Front. Mol. Neurosci. *9*, 30.

Yang, S., Chang, R., Yang, H., Zhao, T., Hong, Y., Kong, H.E., Sun, X., Qin, Z., Jin, P., Li, S., and Li, X.J. (2017). CRISPR/Cas9-mediated gene editing ameliorates neurotoxicity in mouse model of Huntington's disease. J. Clin. Invest. *127*, 2719–2724.

Zeitlin, S., Liu, J.P., Chapman, D.L., Papaioannou, V.E., and Efstratiadis, A. (1995). Increased apoptosis and early embryonic lethality in mice nullizygous for the Huntington's disease gene homologue. Nat. Genet. *11*, 155–163.

Zetsche, B., Volz, S.E., and Zhang, F. (2015). A split-Cas9 architecture for inducible genome editing and transcription modulation. Nat. Biotechnol. *33*, 139–142.